

## Low $pK_a$ Phosphido-Boranes Capture Carbon Dioxide with Exceptional Strength: DFT Predictions Followed by Experimental Validation

Aarya D. Riasati, Charles B. Musgrave III, Nathaniel Yeboah, Aleksandrs Prokofjevs,\* and William A. Goddard III\*

basicity. A few notable exceptions are extremely electron-rich phosphines studied by Dielmann et al.,<sup>6</sup> as well as phosphide metal salts,<sup>7</sup> all of which are exceptionally strong bases. Frustrated Lewis pairs (FLPs), first synthesized by Douglas et al.,<sup>8</sup> have also been analyzed for  $\text{CO}_2$  capture,<sup>9</sup>

itself. Furthermore, analysis of the basicity of these complexes, completed by Dornhaus et al., indicates that the anionic motif of the phosphido-borane salt is more Lewis basic toward the  $[\text{BH}_3]$  compared to its neutral analogues, making these compounds ripe for usage in  $\text{CO}_2$  capture.<sup>11</sup>

with these compounds using a frustrated lone pair induced by steric



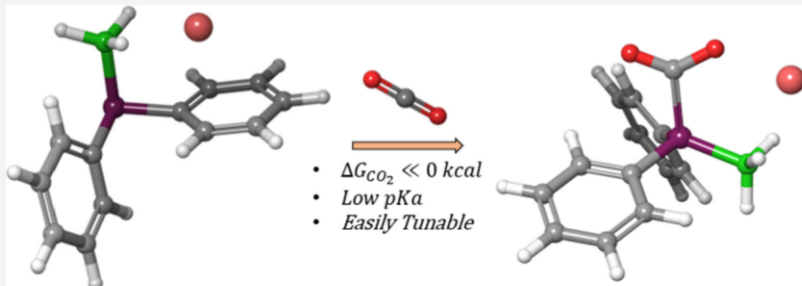
J. Phys. Chem. Lett. 2024, 15, 10909–10917



Read Online

ACCESS |

SI



**ABSTRACT:** We have developed a class of phosphido-boranes (BoPh's) with formula  $X^+[R_2PBH_3^-]$  that bind  $CO_2$  with exceptional strength ( $\Delta G = -8.2$  to  $-24.0$  kcal/mol) at ambient conditions. We use quantum mechanics (QM) to determine how the choice of electron-donating versus electron-withdrawing ligand impacts the  $CO_2$  binding strength, in the presence of a donating borane moiety. We also examine the role of the cation in  $CO_2$  binding, finding that the ion position relative to the bound  $CO_2$  dramatically alters binding strength. We find that the BoPh with two ethyl ligands  $Li[Et_2PBH_3]$  leads to  $\Delta G = -24.0$  kcal/mol upon  $CO_2$  binding while  $Li[Ph_2PBH_3]$  leads to  $\Delta G = -12.8$  kcal/mol. We synthesized the BoPh with two phenyl ligands  $Li[Ph_2PBH_3]$  to validate the QM-predicted stability and predicted  $pK_a$ .

T

1 2

10

simple phosphide complexes are well-established for binding  $CO_2$  and serve as the basis for state-of-the-art  $CO_2$  extraction technologies.<sup>3,4</sup> In contrast phosphines generally do

5

hindrance to drive  $CO_2$  binding. These compounds do not include a P–B bond and instead use steric hindrance to drive binding. While previous analyses have examined various frustrated lewis pairs for  $CO_2$  activation, we find that direct formation of the P–B bond allows for the borane moiety to donate charge to the phosphorus. This allows for these compounds to have extensively different properties than those

Received: August 24, 2024

Revised: October 10, 2024

Accepted: October 14, 2024

Published: October 24, 2024



Herein, we report a combined computational–experimental study that examines several phosphido-boranes (BoPh) for the efficient capture of CO<sub>2</sub>. We used quantum mechanics (QM) to predict CO<sub>2</sub> binding for a number of BoPh's followed by NMR experimental validation in *d*<sub>8</sub>-THF solution. Our deprotonated secondary phosphido-boranes complexes exhibit CO<sub>2</sub> binding free energies of -8.2 to -24.0 kcal/mol at 300 K despite having only moderate Brønsted basicity, comparable to that of the *tert*-butoxide anion. Formation of the Lewis acid–base complex between BH<sub>3</sub> and secondary phosphines (R<sub>2</sub>P–H) leads to a substantial increase in the P–H Brønsted acidity of the H–PR<sub>2</sub>–BH<sub>3</sub><sup>-</sup> adduct compared to the free phosphine. This observation has been exploited widely in the synthesis of tertiary phosphines, since PR<sub>2</sub>–BH<sub>3</sub><sup>-</sup> anions serve as excellent P nucleophiles, bear a built-in BH<sub>3</sub> protecting group for the P atom, and offer significant experimental advantages compared to the parent R<sub>2</sub>P<sup>-</sup> phosphide counterpart.<sup>12</sup> These phosphideborane salts have excellent CO<sub>2</sub> binding in comparison to other P-based systems as a result of their acidity. Instead of a strong base needed for deprotonation and subsequent activation, only mild conditions are needed. While these phosphido-borane complexes have some ditopic character, with dual reactivity at both the P and H centers, the use of these phosphideborane complexes as hydride sources has not been reported. As shown by Consiglio et al.,<sup>12</sup> the introduction of various carbonyl derivatives led to the formation of multiple products due to the inclusion at both the P site and H site in the compounds under investigation. This ditopic behavior indicates the complexity of the reaction mechanisms associated with reduction induced by various phosphideborane compounds.<sup>13</sup> What has so far remained unnoticed is that the PR<sub>2</sub>BH<sub>3</sub><sup>-</sup> anions possess remarkably strong CO<sub>2</sub> binding affinity for P-based compounds with Brønsted basicity between that of bulky trialkylphosphines (e.g., PCy<sub>3</sub>) and the weakest of the P superbases, such as Verkade's base, neither of which form stable CO<sub>2</sub> adducts. Furthermore, the CO<sub>2</sub> binding motif in the form of a single P–C bond in the resulting carboxylate ion rather than a cyclic lactone is likely to benefit subsequent activation to form stable CO<sub>2</sub>-based compounds.

We report here density functional theory (DFT) studies examining several subclasses of phosphido-boranes (BoPh) candidates for use in CO<sub>2</sub> capture. We found that the  $\Delta G$  of CO<sub>2</sub> binding ranges from -8.2 to -24.0 kcal/mol. Of the molecules studied, the BoPh with two phenyl ligands Li[Ph<sub>2</sub>PBH<sub>3</sub>] led to a predicted  $\Delta G = -12.8$  kcal/mol, which we have now validated experimentally.

We first evaluated the influence of electron-withdrawing and electron-donating groups on CO<sub>2</sub> capture and their

interplay with the anionic borane motif. We also investigated the countercation effect on CO<sub>2</sub> capture, revealing how the position of the cation relative to the BoPh dramatically alters CO<sub>2</sub> binding strength. We propose several BoPh's with varying functionalities that may affect CO<sub>2</sub> binding. BoPh's 1, 2, and 3 contain electron-donating groups, and BoPh 4 contains an electron-withdrawing group. Phosphines 5 and 6 do not contain the borane moiety, serving as references for comparison with BoPh's 1 through 4. While it is known that simple phosphide salts form CO<sub>2</sub> complexes, we included example phosphines as reference to explore the effect of the borane unit on CO<sub>2</sub> binding energies. This is shown in the case of phosphine 5.

- 1 [(CH<sub>3</sub>)<sub>2</sub>PBH<sub>3</sub>] contains two –CH<sub>3</sub> (Me) groups which should function as weak electron-donating groups. •
- 2 [(CH<sub>3</sub>CH<sub>2</sub>)<sub>2</sub>PBH<sub>3</sub>] contains two –CH<sub>2</sub>CH<sub>3</sub> (Et) groups, as an extension to 1.
- 3 [(Butyl)<sub>2</sub>PBH<sub>3</sub>] contains the BoPh anion (P–BH<sub>3</sub><sup>-</sup>) accompanied by two *n*-butyl units bound to the central P. Butyl is used here because we previously found that both Me and Et groups had extremely exergonic CO<sub>2</sub> binding strength (-23.1 and -24.0 kcal/mol). Moreover, we can directly compare the butyl groups to the Me and Et groups for CO<sub>2</sub> binding, in the context of altering the chain lengths of unsubstituted alkyl groups to an electron-rich substrate such as the BoPh.
- 4 [(Ph)<sub>2</sub>PBH<sub>3</sub>] has two –C<sub>6</sub>H<sub>5</sub> (Ph) units, which should operate as electron-withdrawing groups bonded to the central, electron-rich P.
- 5 [(Ph)<sub>2</sub>P] also has two Ph units but lacks the borane, such that the third ligand position becomes occupied by the countercation.
- 6 [Ph<sub>3</sub>P] also lacks the borane and should therefore serve nicely for elucidating the effect of the borane moiety on CO<sub>2</sub> binding affinity.

The reactant conformer was selected by varying the position of the counterion across multiple local pockets in the reactant complex. From there, the ion position that led to the lowest-energy conformation was selected. CO<sub>2</sub> binding free energies for the lowest-energy reactant and product conformers with Li<sup>+</sup> counterions are shown in Figure 1. It was observed that the

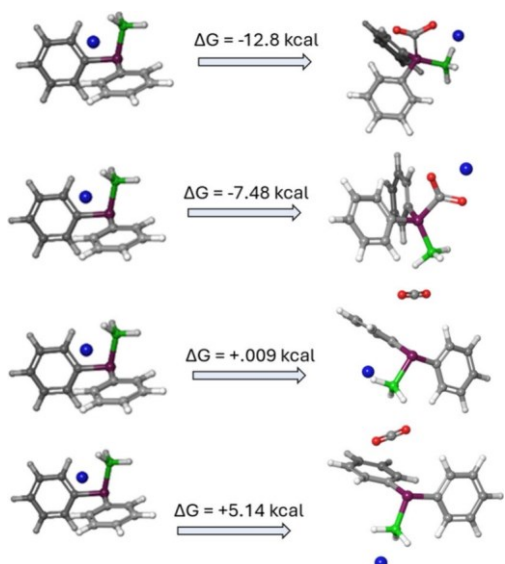


Figure 1. Effect of the counterion on overall  $\Delta G$ . The most stable of the counterion is in-between the  $\text{CO}_2^-$  and  $\text{P-BH}_3$  groups. Moving the counterion to other groups, such as near the  $-\text{BH}_3$  or the  $-\text{CO}_2^-$  groups, drives  $\Delta G$  significantly, to  $-7.5$  and  $+5.1$  kcal, respectively.

closer the counterion was to the  $\text{P-BH}_3$  unit, the more able it was to stabilize charge and thus the more effectively it was able to substantially increase reactant stability.

The overall  $\Delta G$  of binding  $\text{CO}_2$  is based on the stability of the product complex. The counterion plays a significant role in stabilizing the  $\text{CO}_2^-$  moiety upon binding, balancing charge distribution throughout the entire system. Altering the placement of the counterion in different pockets

For the case of  $\text{Li}^+$  counterions, the most stable product  $\text{BoPh}$  conformer has the  $\text{Li}^+$  seated between an oxygen of the bound  $\text{CO}_2$  and two hydrides of the anionic  $-\text{BH}_3^-$ . Increases in the thermodynamic driving force as a result of this can be attributed to charge stabilization in the product

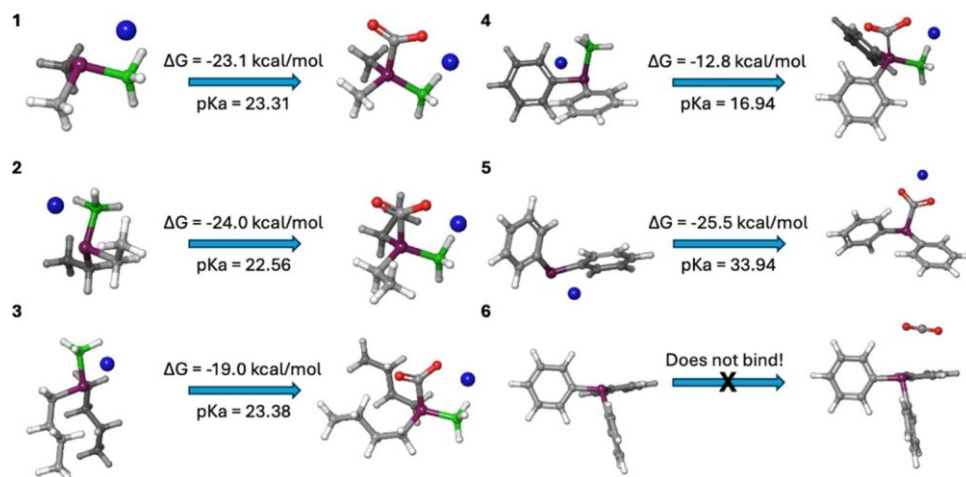


Figure 3. DFT-predicted  $\text{CO}_2$  binding energies (kcal/mol) in THF solvent with  $\text{Li}$  counterions for various  $\text{BoPh}$ 's. Here P is purple, B is green, C is gray, H is white, and Li is blue.  $pK_a$  values were tabulated in water solvent, following the equation  $pK_a = \frac{1}{2.3RT}D$ , where  $D$  is the free energy change  $\Delta G_{\text{CO}_2} = -12.8 \text{ kcal}$



Figure 2. Effect of distance on  $\Delta G$ . Increasing the counterion distance from the  $\text{O-BH}_3$  pocket by  $0.35 \text{ \AA}$  increases binding energy by  $+5.9 \text{ kcal}$ .  $\Delta G_{\text{CO}_2}$  increases for the biphenyl case from  $-12.8 \text{ kcal/mol}$  to  $-6.9 \text{ kcal/mol}$ .

associated with dissociation of  $\text{BH}^+$  to  $\text{B}^-$  and  $\text{H}^+$  in water solvent. The value of  $\text{H}^+$  is determined to be  $-259.5 \text{ kcal/mol}$  for the solvation free energy change of a proton.

throughout the system dramatically changes binding energies. Here, the closer the counterion is to the bounded  $\text{CO}_2$  and the electronrich moieties of the system, including the electron-donating  $-\text{BH}_3$  unit, the more able it is to stabilize effective charge. Shown in the following, a summary of the effect of the counterion in terms of overall binding energies is presented by changing the pocket where each counterion is coordinated to the system. As shown in the image, the pocket where the counterion is coordinated to the system dramatically affects binding energy.

Absolute distance also affects binding energy. In the first case, where the  $\text{Li}^+$  counterion is positioned between the terminal oxygen and the  $-\text{BH}_3$  group, increasing the distance by merely  $0.35 \text{ \AA}$  increases binding energy by  $+5.9 \text{ kcal}$ . This is shown in Figure 2.

structure, as well as charge transfer from P to the  $\text{CO}_2$  unit upon binding.<sup>14</sup> In these structures, binding  $\text{CO}_2$  leads the borane moiety to donate a charge of  $+0.09$  to the P-C single bond (P is now formally +1). We generally find that bulkier ligands increase steric crowding which in turn limits the availability of the nucleophilic P for binding  $\text{CO}_2$ .

As shown for compound 4, the coupled effect of having both weak electron-withdrawing groups and steric crowding around the nucleophilic site of the phosphorus lone pair decreases the magnitude of  $\Delta G$ , although the anionic borane offsets this effect due to charge transfer into the newly formed P-C bond. In compounds 1, 2, and 3, alkyl groups act as weak electron donors to the nucleophilic P binding site, leading to  $\Delta G$  from  $-24$  to  $-19 \text{ kcal/mol}$  (Figure 3).

In BoPh 4, the reactant P charge is much higher than those of BoPh 1–3. The larger cationic character of the phosphorus in the reactant complex limits the ability for nucleophilic attack on the electrophilic carbon of the  $\text{CO}_2$ , decreasing the  $\Delta G$  to  $-13$  kcal/mol. Compared to other conformers in which the counterion was placed in less stable sites,  $\text{Li}^+$  coordination to the oxygen of the  $\text{CO}_2$  unit and the hydrides of the borane (Figure 1) yielded O–C–O bond angles close to  $\text{sp}^2$  hybridization ( $120^\circ$ ). Strong deviation from the linear bond angle of  $180^\circ$  for  $\text{CO}_2$  also indicates increased thermodynamic driving force for  $\text{CO}_2$  binding, with more negative  $\Delta G$  values arising from species able to accommodate  $\text{CO}_2$  near  $120^\circ$ . As the  $\text{Li}^+$  moves closer to the oxygens, the O–C–O bond angle decreases to near the  $\text{sp}^2$  hybridization angle of  $120^\circ$ .

$\text{Li}^+$ , along with its role in adjusting the  $\text{CO}_2$  bond angle, acts as a soft Lewis acid in the THF solvent, making  $\Delta G$  more negative. The naked biphenyl phosphide-borane has an incredibly downhill binding energy of almost  $-12$  kcal/mol for  $\text{CO}_2$  binding. Other analogues have even stronger

This would ultimately balance adsorption and collection  $\Delta G$ s for capture and subsequent conversion.

Explicit solvent inclusion in the reactant conformers indicates that, in addition to stabilizing effects from both the phosphorus (P) and boron (B) atoms due to the counterion being placed between them, the electron-donating tetrahydrofuran (THF) molecules also contribute to stabilization. The oxygens of each THF group are oriented toward the counterion, enhancing the overall stability of the system. This has been validated through X-ray crystallography of the reactant structures and is in direct agreement with previous analyses of these phosphido-borane complexes in THF and other electron-donating solvents.<sup>10,12</sup> However, while inclusion of these stabilization effects is necessary for understanding the system, they are minimal in their effect on  $\text{CO}_2$  capture. The additional stability provided by the THF groups only increases  $\Delta G$  of  $\text{CO}_2$  binding by  $3.0$  kcal/mol. This has been elucidated in comparing  $\text{CO}_2$  binding in  $[(\text{Ph})_2\text{PBH}_3]$  using DFT. This is shown in Figure 4.

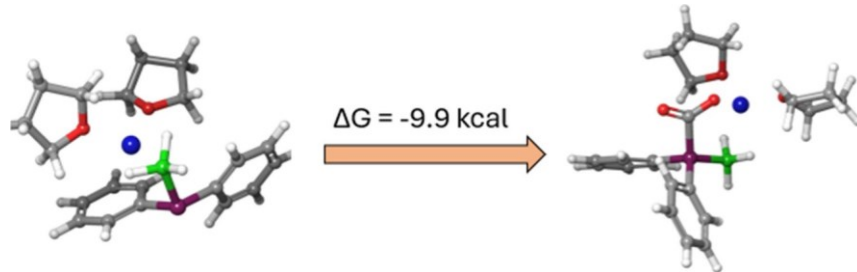


Figure 4. Explicit solvation of the  $[(\text{Ph})_2\text{PBH}_3]$  phosphido-borane. Explicit solvation increases overall  $\Delta G$  by  $+2.9$  kcal/mol, but it is still bound by  $9.9$  kcal/mol.

binding energies, some in the  $-20$  to  $-30$  kcal/mol range. This result can be used as a baseline for further alterations to the ligands bound to phosphorus to increase overall  $\Delta G$  for conversion to a value-added product. For the creation of a value-added product,  $\Delta G$  for  $\text{CO}_2$  binding must be increased in order to ensure that the bound  $\text{CO}_2$  can be released upon formation of the product. This can be done in a variety of different ways, including the following:

- decreasing the nucleophilicity of the phosphorus by increasing the electron-withdrawing nature of the ligands, e.g., by introducing  $-F$  substituents on the aryl withdrawing group or otherwise;
- decreasing the electron-donating ability of the  $-\text{BH}_3$  group by replacing the hydrides with other substituents;
- altering reaction conditions to make conditions more acidic; or
- changing the counterion involved in stabilizing the bound  $\text{CO}_2$  product, such as replacing  $\text{Li}^+$  with  $\text{K}^+$ .

In regard to the effect of the counterion on  $\text{CO}_2$  stability, while the charge of the  $\text{Li}^+$  counterion remains unchanged in compounds 1 through 5,  $\text{Li}^+$  polarizes the oxygens of the  $\text{CO}_2$  unit in the product, slightly disrupting otherwise perfect resonance among both O atoms of the  $\text{CO}_2$ -bound complex.

The  $\text{p}K_a$  of the phosphido-borane conjugate acid is correlated to the binding affinity of  $\text{CO}_2$  to the central phosphorus, with higher  $\text{p}K_a$  values indicating a greater Lewis basicity and hence greater reactivity to the Lewis acidity of the  $\text{CO}_2$ . This can be seen in differences between phosphines 1, 2, and 3, with  $\text{p}K_a = 23$ , and 4, with  $\text{p}K_a = 17$ . The relative acidity of the  $\text{H}-\text{P}^+\text{R}_2\text{BH}_3^-$  complex compared to the naked  $\text{H}-\text{PPh}_2$  requires only a mild base to form the active lone pair site on the phosphorus. Here, the borane moiety increases the acidity of the hydrogen on the  $\text{H}-\text{P}^+\text{R}_2\text{BH}_3^-$  zwitterionic complex acting as a source of electron charge upon  $\text{CO}_2$  binding, effectively making  $\Delta G$  less negative and increasing synthetic ease.

Along with the correlation of the O–C–O bond angle with  $\Delta G$  values, the zwitterion character changes. While no

conclusions can be made about the correlation between zwitterionic character and the thermodynamic driving force of  $\text{CO}_2$  binding, zwitterion formation may provide insight as to the mechanism of binding and the origin of such high  $\Delta G$  values. The  $\text{BH}_3^-$  group present in each BoPh complex acts as a source of electron density upon  $\text{CO}_2$  binding, with the Lewis basicity of each P atom increasing upon binding due to the donation of charge from the  $\text{BH}_3^-$  moiety. Replacing the  $\text{BH}_3^-$  moiety with the  $-\text{R}$  group ligand decreases the  $\Delta G$  values for all tested species. Replacing  $\text{BH}_3^-$  with  $-\text{Ph}$ , as shown for 6, increased  $\Delta G$  of  $\text{CO}_2$  binding significantly, to the point where  $\text{CO}_2$  binding was no longer favorable.

For comparison, we also computed  $\text{CO}_2$  binding strengths in the presence of a  $\text{Na}^+$  counterion. Reactant and product structures along with their respective  $\text{CO}_2$  binding energies are depicted in [Figure S1 of the Supporting Information](#).

$\text{Na}^+$  is a softer ion than  $\text{Li}^+$  in terms of its cationic character. As a result, charge stabilization in the  $\text{Na}^+$  product complex is not as pronounced as for the  $\text{Li}^+$  case. Lack of stabilization in the product conformer reduces the stability of the product complex, making  $\Delta G$  less negative, as illustrated in [Figure S1](#). Decreased charge stabilization in the product complex also increases the transition state barrier ( $\Delta G^\ddagger$ ) for  $\text{CO}_2$  binding. In both the  $\text{Na}^+$ - and  $\text{Li}^+$ -containing transition states, the counterion is positioned between the approaching  $\text{CO}_2$  and the  $\text{BH}_3^-$  moiety of the phosphido-boranes. The counterion forms an ion pair with the negatively charged  $\text{BH}_3^-$  subunit, simultaneously accepting charge from the partially charged oxygens of the now-binding  $\text{CO}_2$ . In addition, the decreased polarization in the transition state reduces the overall energy of the system, reducing the large differences in polarization in the activated complex. Decreased charge polarization subsequently reduces the transition state energy and thus the overall activation barrier.

The transition state and binding free energies for  $[(\text{Ph})_2\text{PBH}_3]$  with  $\text{Li}^+$  and  $\text{Na}^+$  are depicted in [Figure 5](#); here, the position of the counterion is of critical importance. In [Figure 5](#), we observe that  $\text{Li}^+$  coordinated to a  $\text{CO}_2$  oxygen and the hydrides of the  $\text{BH}_3^-$  reduces  $\Delta G^\ddagger$  by  $\sim 2$  kcal/mol relative to  $\text{Na}^+$ . The overall  $\text{CO}_2$  binding  $\Delta G^\ddagger$  values for the  $\text{Li}^+$ - and  $\text{Na}^+$ -containing phosphido-boranes are +2.43 and +4.43 kcal/mol, respectively. The  $\Delta G^\ddagger$  values of  $\text{CO}_2$  binding for the parent  $\text{Li-PPH}_2$  and  $\text{Na-PPH}_2$  which lack the borane are +0.7 and +1.5 kcal/mol, respectively.

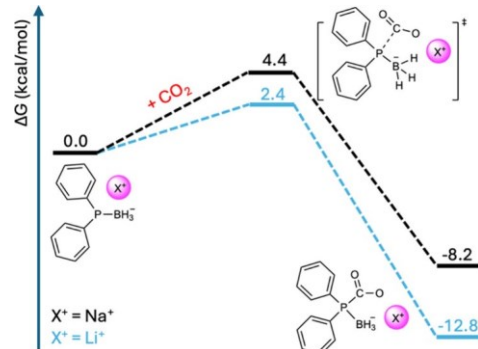


**Figure 5.** DFT-predicted binding and transition state energies at 300 K for the  $\text{Li}$  and  $\text{Na}$ -containing diphenylphosphido-boranes in THF solvent. The pink  $\text{X}^+$  indicates the counterion. The blue and black paths indicate the potential energy surfaces for  $\text{Li}^+$  and  $\text{Na}^+$ , respectively.

While direct pathways of  $\text{CO}_2$  binding are almost instantaneous, competing  $\text{BH}_3$  transfer reactions must also be considered.  $\text{BH}_3^-$  transfer from  $\text{THF-BH}_3$  to  $\text{PPh}_2\text{BH}_3$  for the formation of  $\text{Na}^+\text{PPh}_2(\text{BH}_3)_2$  is unfavorable in comparison to  $\text{CO}_2$  binding, with a  $\Delta G^\ddagger$  of +9.6 kcal/mol. Formation of  $\text{Na}^+\text{PPh}_2\text{BH}_3^-$  via  $\text{BH}_3$  transfer from  $\text{BH}_3\text{THF}$  to  $\text{Na}^+\text{PPh}_2^-$  in the absence of  $\text{CO}_2$  occurs with a barrier of +10.9 kcal/mol; this reaction occurs instantaneously in experiment (see below).

In addition to  $\text{Na}^+$  and  $\text{Li}^+$ ,  $\text{PPh}_4^+$  was also used as a counterion in our experiments. Because of the bulky and rigid nature of  $\text{PPh}_4^+$ ,  $\text{CO}_2$  was unable to bind to the phosphidoboranes complex, with  $\text{PPh}_4^+$  forming a salt complex with the reactant phosphine instead. This, alongside [Figure 1](#) and [Tables 1](#) and [S1](#), highlights the significance of the counterion in binding. To separately control the transition barrier and adsorption energy, alterations to the counterion and the system can be done separately to alter one or the other. As shown in the figure, substituting  $\text{Li}^+$  for  $\text{Na}^+$  increases  $\Delta G$  of adsorption while only slightly increasing the transition state barrier. This decreases the stability of the product complex without necessarily affecting the transition state barrier significantly. Similarly, if one were to use a sterically hindered counterion, such as a quaternary carbon or nitrogen, one could raise the transition state barrier while keeping the binding energy unchanged. The phosphorus would be unavailable to attack the Lewis acidic  $\text{CO}_2$ , and thus, the activation energy would increase without necessarily altering the binding energy if an equivalently stabilizing counterion were to be used. Adjusting either the ligand or the counterion in regard to steric control and counterion alterations could selectively adjust either the transition state barrier or the adsorption energy, respectively. To shed further insight on the role of the

counterion and electron-donating and electron-withdrawing groups in  $\text{CO}_2$  binding, we examined additional phosphine complexes with other donating and withdrawing ligands, as shown in Figure 3 and Table 2.

- $(\text{CH}_3\text{O})_2\text{PBH}_3$  (Figure 6, 1) contains two  $-\text{CH}_2\text{OH}$  units, which should operate as weak electron-withdrawing groups. The position of the oxygen atoms in the methoxy groups stabilize the counterion, decreasing  $\text{CO}_2$  binding.
- $\text{F}_2\text{PBH}_3$  (Figure 6, 2) has two  $-\text{F}$  groups. The F explores the effects of an inductive electron-withdrawing group. The  $-\text{F}$  R-group withdraws electron density away from the nucleophilic phosphorus atom. This makes  $\Delta G$  significantly less negative.
- $(\text{F}_5\text{C}_6)_2\text{PBH}_3$  (Figure 6, 3) has two  $-\text{C}_6\text{F}_5$  groups, acting as electron-withdrawing aryl groups, again removing charge from the P and leading to much less favorable  $\Delta G$ .
- $(\text{TMG})_2\text{PBH}_3$  (Figure 6, 4) contains the phosphidoBorane anion ( $\text{P}-\text{BH}_3^-$ ) accompanied by two monodentate tetramethyl guanidium (TMG) ligands bound to the central P. TMG is used here because we previously found that  $\text{P}(\text{TMG})_3$ <sup>15</sup> had a very exergonic  $\text{CO}_2$  binding strength ( $-13.5$  kcal/mol); however, here  $\Delta G = -7.4$  kcal/mol.
- $[(\text{H}_3\text{C})_2\text{N}]_2\text{PBH}_3$  (Figure 6, 5) contains two  $-\text{N}$ -

$(\text{CH}_3)_2$  ligands which act as electron-donating groups to the nucleophilic phosphorus, leading to  $\Delta G = -14.3$  kcal/mol.

As found in the alkyl BoPh's,  $\Delta G$  is correlated to  $\Delta Q$  on P. Cases with the more negative  $\Delta G$  have larger  $\Delta Q$  values, regardless of whether the ligand type present is electrondonating or electron-withdrawing. However, electron-donating groups on the phosphine did yield lower  $\Delta G$  values than electron-withdrawing groups, highlighting the significance of ligand choice in BoPh synthesis. Higher negative charge on the  $\text{CO}_2$  moiety is correlated with a lower  $\Delta G$ . Interestingly, smaller values of  $\Delta Q$  on  $\text{BH}_3^-$  are correlated with lower  $\Delta G$  values.  $(\text{F}_5\text{C}_6)_2\text{PBH}_3$ , with two electron-withdrawing  $\text{C}_6\text{F}_5$  groups, exhibits a large change in  $\Delta Q$  upon  $\text{CO}_2$  binding. Contrasted with  $[(\text{H}_3\text{C})_2\text{N}]_2\text{PBH}_3$  containing two electrondonating  $-\text{N}(\text{CH}_3)_2$ ,  $\Delta Q$  on  $\text{BH}_3^-$  in  $(\text{F}_5\text{C}_6)_2\text{PBH}_3$  was significantly higher, by  $+0.08$ . This trend is not observed in the alkyl and aryl BoPh's, indicating that electron-donating and electron-withdrawing ligand groups drastically impact the ability of  $\text{BH}_3^-$  to donate charge and stabilize the  $+1$  charge on phosphorus.  $\Delta Q$  is the change in the charge on the phosphorus and  $-\text{BH}_3$  moieties, upon formation of the  $(+1)$  tetravalent phosphorus upon binding of the  $\text{CO}_2$ . A higher  $\Delta Q$  is indicative of the relative nucleophilicity of the phosphorus in context of a potent Lewis acid such as  $\text{CO}_2$ . In the case of  $\text{CO}_2$  binding, if  $\Delta Q$  is larger, then the reactant is very nucleophilic and is able to bind  $\text{CO}_2$  easier as compared to compounds where  $\Delta Q$  is far smaller. For  $\text{BH}_3$ , upon binding  $\text{CO}_2$ , charge is

Table 1. Properties of Various BoPh's<sup>a</sup>

Phosphido-borane	$\Delta G$ of $\text{CO}_2$ binding	$\Delta Q$ on P	$\Delta Q$ on $\text{BH}_3^-$	$\text{CO}_2$ Charge	Change in P-B Bond Order	P-C Bond Order
$[(\text{CH}_3)_2\text{PBH}_3]$	-23.1	+0.73	+0.088	-0.992	-0.067	+0.82
$[(\text{CH}_3\text{CH}_2)_2\text{PBH}_3]$	-24.0	+0.74	+0.086	-0.970	-0.074	+0.81
$[(\text{Butyl})_2\text{PBH}_3]$	-19.0	+0.72	+0.082	-0.987	-0.079	+0.84
$[(\text{Ph})_2\text{PBH}_3]$	-12.8	+0.57	+0.082	-0.942	-0.061	+0.84

<sup>a</sup>For the case of a  $\text{Li}^+$  counterion in THF.  $\text{CO}_2$  binding free energy (kcal/mol), charges on the P atom and  $\text{BH}_3^-$  moiety in both reactant and product complexes, O-C-O bond angle after binding, and P-B and P-C bond orders (BO) and bond lengths (Å).

Table 2. Binding Energy of  $\text{CO}_2$  Binding and Respective Charges on the P Atom and  $\text{BH}_3^-$  Moiety or the  $\text{Li}^+$  Counterion in THF in Both Reactant and Product Complexes P-B and P-C Bond Orders<sup>a</sup>

Phosphido-borane	$\Delta G$ of $\text{CO}_2$ binding	$\Delta Q$ on P	$\Delta Q$ on $\text{BH}_3^-$	$\text{CO}_2$ Charge	Change in P-B Bond Order	P-C Bond Order
$(\text{CH}_3\text{O})_2\text{PBH}_3$	-7.6	+0.74	+0.06	-1.03	-0.09	+0.78
$\text{F}_2\text{PBH}_3$	-1.3	+0.65	+0.02	-0.96	-0.11	+0.82
$(\text{F}_5\text{C}_6)_2\text{PBH}_3$	-0.4	+0.49	+0.11	-0.85	-0.07	+0.84
$(\text{TMG})_2\text{PBH}_3$	-7.4	+0.78	+0.01	-1.09	-0.02	+0.73
$[(\text{H}_3\text{C})_2\text{N}]_2\text{PBH}_3$	-14.3	+0.77	+0.03	-1.03	-0.05	+0.78

<sup>a</sup> $\Delta G$  of  $\text{CO}_2$  binding and  $\Delta Q$ 's are shown here as well. The

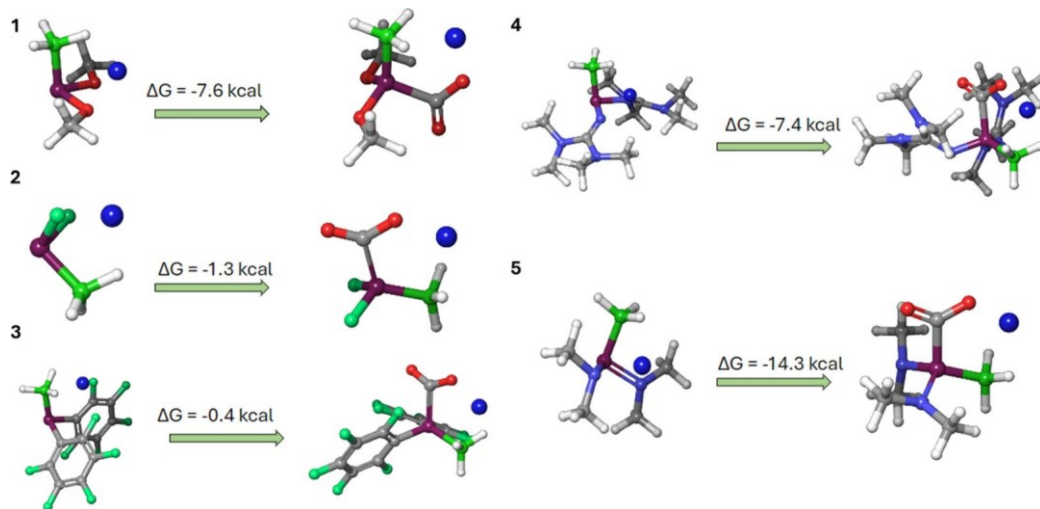


Figure 6. DFT-predicted  $\text{CO}_2$  binding energies (kcal/mol) in THF solvent with Li counterions for various BoPh's. Here P is purple, B is green, C is gray, H is white, Li is dark blue, N is light blue, O is red, and F is turquoise.

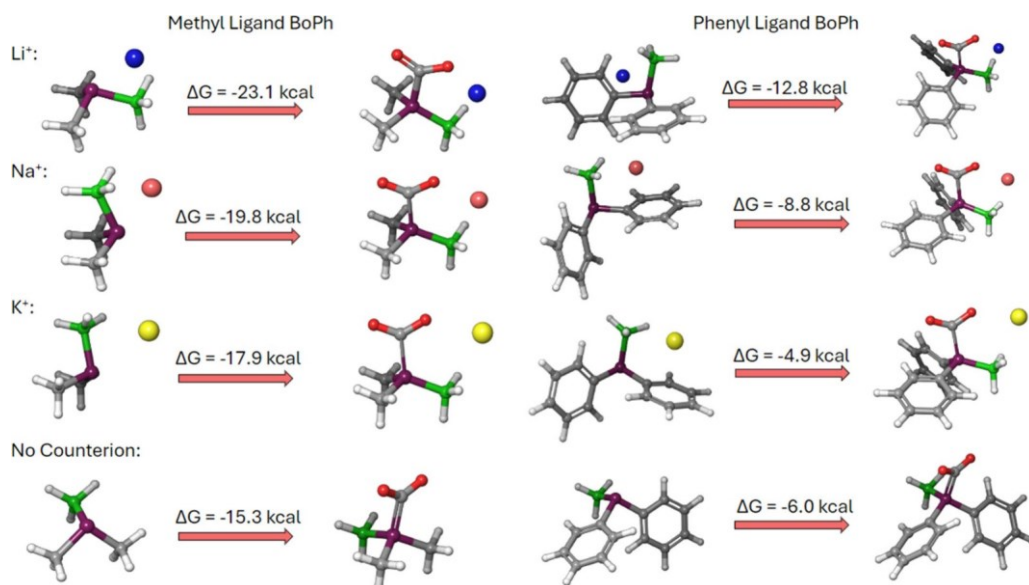


Figure 7. DFT-predicted  $\text{CO}_2$  binding energies (kcal/mol) in THF solvent with methyl and phenyl BoPh's with no counterion, and with  $\text{Li}^+$ ,  $\text{Na}^+$ , and  $\text{K}^+$ . Here P is purple, B is green, C is gray, H is white, Li is dark blue, Na is pink, K is yellow, and O is red.

donated from the  $\text{BH}_3$  to the P–C bond. This increases  $\Delta G$  and is what is responsible for the incredibly high  $\Delta G$  values shown here.

Electron-donating groups increase the nucleophilicity and electron density on the phosphorus, increasing its ability of nucleophilic attack on the electrophilic carbon center of  $\text{CO}_2$ . This then decreases  $\Delta G$ . Electron-withdrawing groups decrease the electron density at phosphorus and hence its nucleophilicity. This then decreases the magnitude of  $\Delta Q$  on P, resulting in smaller overall change in electron density between product and reactant structures. In addition to charge density, there is a correlation between bond order and  $\Delta G$ . BoPh's with little to no difference in reactant and product P–B bond orders have more negative  $\Delta G$  values, as

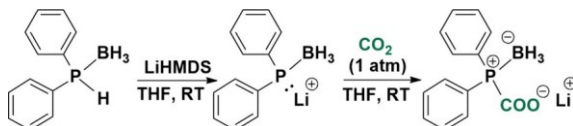
opposed to BoPh's with larger differences in P–B bond orders. The resulting difference between the product and reactant conformers is also responsible for increased  $\Delta G$  values. As a result of the increased stability of the  $\text{Li}^+$  counterion in the  $(\text{TMG})_2\text{PBH}_3$  complex from the nitrogens, the reactant complex is more stable than it otherwise would be without the nitrogens. This then decreases overall reactivity and increases  $\Delta G$ .

The counterion stabilizes effective charge buildup in both the product and transition state, resulting in more negative overall  $\Delta G$  values. Furthermore, changes in the relative size of the counterion drastically affect  $\Delta G$ , as shown for the  $\text{Li}^+$ ,  $\text{Na}^+$ , and  $\text{K}^+$  cases in Figure 7. As shown below, increasing counterion size increases  $\Delta G$  of binding.

The counterion stabilizes charge in the product and transition state, making  $\Delta G$  more negative. Here, we see that due to the larger size of  $\text{Na}^+$ , it is unable to stabilize charge as well as  $\text{Li}^+$ . This is also seen for  $\text{K}^+$ . In addition, for the no counterion cases with methyl and phenyl R-groups, there is no stabilization of charge in the entire anionic complex, with  $\Delta G$  hence being the most positive. Between  $\text{Li}^+$  and the cases with no counterion, we see a large difference in  $\Delta G$ . Thus, between the methyl and phenyl cases,  $\Delta G$  increases by an average of +7.3 kcal.

**Experiments.** Very few studies have been published on phosphine-based systems that bind  $\text{CO}_2$ .<sup>16–18</sup> These systems either exhibit very strong basicity or create electron density on the P atom, making it electron-rich. For instance, the work of Buß et al. showcases electron-rich phosphines that bind  $\text{CO}_2$ , where their most stable adducts or best phosphines have predicted  $\text{p}K_a$  value of  $\sim 33.7$  and free binding energy at room temperature of  $-10.3$  kcal/mol.<sup>16</sup> In contrast, our BoPh's have predicted binding free energies up to 23 kcal/mol with  $\text{p}K_a$  as low as 17. To validate our computational studies, we synthesized the anionic diphenylphosphido-borane, 4, since it had the lowest  $\text{p}K_a$  and a good binding energy (Scheme 1).

Scheme 1



First we synthesized the diphenylphosphine  $\text{Li}[\text{Ph}_2\text{PBH}_3]$  borane complex by following the synthetic route described by Stankevic et al.<sup>19</sup> Here 0.2218 g of the resulting phosphidoborane was dissolved in 3 mL of tetrahydrofuran (THF) in a 10 mL valve. Here 2 mL of THF was used to dissolve 0.1856 g of lithium bis(trimethylsilyl)amide (LiHMDS). The solution of LiHMDS was added dropwise to the solution of

$\text{Li}[\text{Ph}_2\text{PBH}_3]$  to minimize side reactions. An aliquot of the resulting solution was taken to confirm the structure using NMR spectroscopy with the results in Figure 8b, confirming complete deprotonation  $\text{Li}[\text{Ph}_2\text{PBH}_3]$  to form  $\text{Li}[\text{Ph}_2\text{PBH}_3]$  salt. We then bubbled  $\text{CO}_2$  gas through lithiated anionic phosphido-borane salt at 1 atm and room temperature for about 10 min to saturate it with  $\text{CO}_2$ . NMR analysis on an aliquot of the sample revealed formation of P- $\text{CO}_2$  adducts as shown in Figure 8c. For confirmation of the predicted  $\text{p}K_a$  of the P  $\text{Li}[\text{Ph}_2\text{PBH}_3]$ , we used lithium tertbutoxide to deprotonate the  $\text{Li}[\text{Ph}_2\text{PBH}_3]$  in butanol which resulted in the lithiated anionic phosphido-borane salt. This leads to a  $\text{p}K_a$  of 19.2, in good agreement with the predicted  $\text{p}K_a$  of 21.3 for

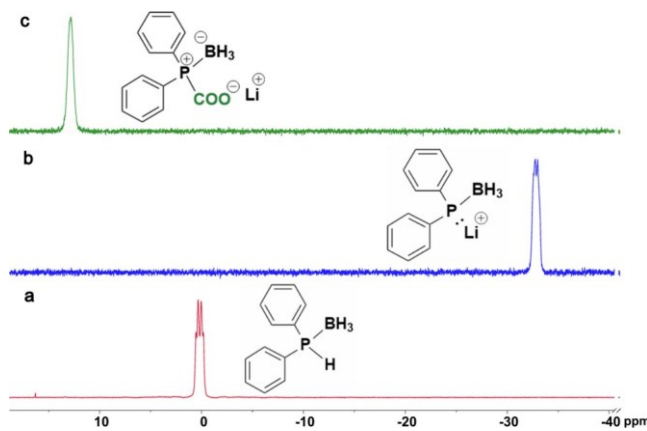


Figure 8. (a)  $^{31}\text{P}$  NMR of  $\text{Li}[\text{Ph}_2\text{PBH}_3]$  (red spectrum) (162 MHz,  $\text{THF}-d_8$ )  $\delta$  1.16 to  $-0.79$  (m). (b)  $^{31}\text{P}$  NMR of  $\text{LiPh}_2\text{PBH}_3$  (blue spectrum), (162 MHz,  $\text{THF}-d_8$ )  $\delta$   $-32.87$  (d,  $J = 60.7$  Hz). (c)  $^{31}\text{P}$  NMR of  $\text{LiPh}_2\text{PBH}_3-\text{CO}_2$  (green spectrum) (162 MHz,  $\text{THF}-d_8$ )  $\delta$  12.86.

lithium tert-butoxide, which is consistent with the lower  $\text{p}K_a$  of 17 for  $\text{Ph}_2\text{BoPh}$ .

Figure 8 shows the  $^{31}\text{P}$  NMR resonance spectra of  $\text{Ph}_2\text{BoPh}$  (Figure 8a),  $\text{Li}[\text{Ph}_2\text{PBH}_3]$  salt (Figure 8b), and the  $\text{Li}[\text{Ph}_2\text{PBH}_3]-\text{CO}_2$  adduct (Figure 8c). The spectra in Figure 8a,b show a quartet resonance signal due to  $^{31}\text{P}-^{11}\text{B}$  coupling. The upfield chemical shift from 0.19 ppm to  $-32.87$  ppm indicates successful deprotonation of the phosphido-borane complex to form its lithiated salt. This upfield shift is expected as a result of the shielding effect of the lone pair on the phosphorus atom, which is very much in accordance with the works by Jaska et al.<sup>20</sup> The downfield chemical shift from  $-32.87$  ppm to 12.86 ppm in Figure 8c due to the  $\text{CO}_2$  molecule bound to the phosphorus atom results from deshielding of the phosphorus nuclei by the Lewis acid, which in this case is the  $\text{CO}_2$  gas molecule. The broad characteristic peak feature of the  $^{31}\text{P}$  NMR of the  $\text{Li}[\text{Ph}_2\text{PBH}_3]-\text{CO}_2$  adduct is likely the result of an exchanging of the  $\text{CO}_2$  from one phosphorus atom to another.

Figures 9 and 10 depict the  $^1\text{H}$  and  $^{13}\text{C}$  NMR of the  $\text{Ph}_2\text{PBH}_3$  (red spectrum),  $\text{LiPh}_2\text{PBH}_3$  (blue), and  $\text{LiPh}_2\text{PBH}_3-\text{CO}_2$  (green spectrum) respectively. The disappearance of the P-H bond at 6.83 and 5.88 ppm in Figure 8 (blue spectrum) shows the complete formation of  $\text{LiPh}_2\text{PBH}_3$  which serves as the nucleophilic material that reacts with  $\text{CO}_2$  to form the  $\text{LiPh}_2\text{PBH}_3-\text{CO}_2$  (green spectrum). As shown in Figure 8 (green spectrum), the P atom does not steal any H from the  $\text{BH}_3$  unit but rather binds successfully with the  $\text{CO}_2$  molecule to form the adduct. This is further confirmed by the  $^{13}\text{C}$  NMR in Figure 10 (green spectrum), where the appearance of the signals at 172.95

and 172.11 ppm shows the coupling of the P atom to the  $\text{CO}_2$  molecule from the  $\text{LiPh}_2\text{PBH}_3\text{-CO}_2$  complex.

In conclusion, in this work, we propose novel, easily synthesized borane-phosphines for  $\text{CO}_2$  capture and sequestration. Along with extremely favorable  $\Delta G$  values of -13 to -23 kcal/mol for  $\text{CO}_2$  binding, only mildly basic conditions are needed for reduction and subsequent deprotonation of  $\text{Li}[\text{Ph}_2\text{PBH}_3]$ . This, along with the inexpensive reagents needed for their synthesis, makes use of these BoPh's for  $\text{CO}_2$  sequestration very appealing.

c

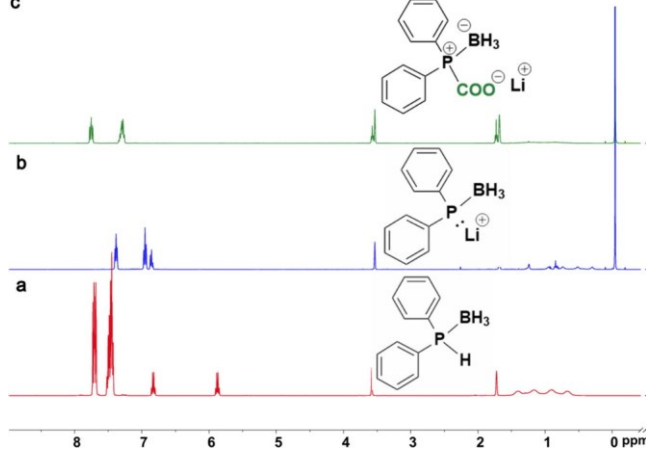


Figure 9.  $^1\text{H}$  NMR of (a)  $\text{Ph}_2\text{PHBH}_3$  (red), (b)  $\text{LiPh}_2\text{PBH}_3$  (blue), and (c)  $\text{LiPh}_2\text{PBH}_3\text{-CO}_2$  (green). (a)  $^1\text{H}$  NMR of  $\text{Ph}_2\text{PHBH}_3$  (red spectrum) (400 MHz,  $\text{THF}-d_8$ )  $\delta$  7.75–7.65 (m, 5H), 7.53–7.40 (m, 7H), 6.83 (q,  $J$  = 7.1 Hz, 1H), 5.88 (q,  $J$  = 7.1 Hz, 1H), 1.04 (dd,  $J$  = 199.4, 94.5 Hz, 4H). (b)  $^1\text{H}$  NMR of  $\text{LiPh}_2\text{PBH}_3$  (blue spectrum) (400 MHz,  $\text{THF}-d_8$ )  $\delta$  7.43 (ddd,  $J$  = 8.0, 6.1, 1.5 Hz, 5H), 7.00 (td,  $J$  = 7.2, 1.3 Hz, 5H), 6.93–6.85 (m, 2H), 0.67 (dd,  $J$  = 174.9, 86.6 Hz, 5H). (c)  $^1\text{H}$  NMR of  $\text{LiPh}_2\text{PBH}_3\text{-CO}_2$  (green spectrum) (400 MHz,  $\text{THF}-d_8$ )  $\delta$  7.80 (ddt,  $J$  = 9.9, 6.7, 1.6 Hz, 5H), 7.41–7.28 (m, 7H), 1.42–0.60 (m, 4H).

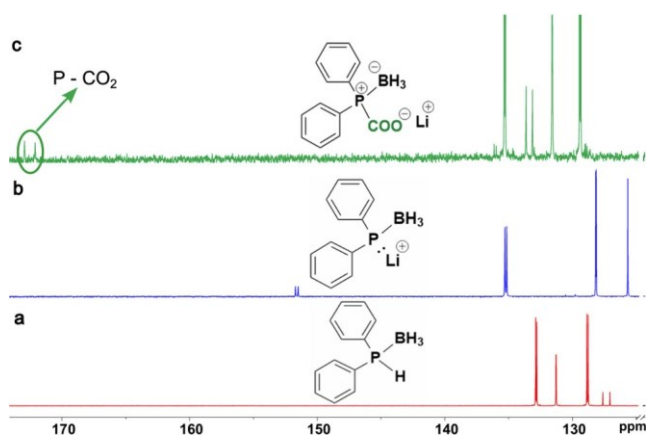


Figure 10.  $^{13}\text{C}$  NMR of (a)  $\text{Ph}_2\text{PHBH}_3$  (red), (b)  $\text{LiPh}_2\text{PBH}_3$  (blue), and (c)  $\text{LiPh}_2\text{PBH}_3\text{-CO}_2$  (green). (a)  $^{13}\text{C}$  NMR of  $\text{Ph}_2\text{PHBH}_3$  (red spectrum) (101 MHz,  $\text{THF}-d_8$ )  $\delta$  132.88, 132.79, 131.29, 131.27, 128.87, 128.76, 66.22, 66.00, 24.15, 23.95. (b)  $^{13}\text{C}$  NMR of  $\text{LiPh}_2\text{PBH}_3$  (blue) (101 MHz,  $\text{THF}-d_8$ )  $\delta$  135.32, 135.17, 128.21, 128.16, 125.68, 68.87, 68.73, 68.51, 26.73, 26.61, 26.53, 26.41, 26.33. (c)  $^{13}\text{C}$  NMR of  $\text{LiPh}_2\text{PBH}_3\text{-CO}_2$  (green spectrum) (101 MHz,  $\text{THF}-d_8$ )  $\delta$  172.95,

172.11, 135.36, 135.28, 131.62, 131.60, 129.47, 129.37, 68.86, 68.73, 68.64, 68.51, 26.74, 26.61, 26.54, 26.41, 26.33.

Counterion effects also play a significant role in binding, with  $\text{Li}^+$  encouraging stronger  $\text{CO}_2$  binding compared to  $\text{Na}^+$  and  $\text{K}^+$ .

In the context of these highly polarized phosphido-borane species, the cationic counterion provides charge stabilization for the product, increasing the magnitude of the  $\Delta G$ . Based on the large negative magnitude of the  $\Delta G$  values predicted, experimental studies in  $\text{CO}_2$  activation to form hydrocarbon products from these phosphido-boranes are warranted.

## COMPUTATIONAL METHODS

All density functional theory calculations were performed using the Jaguar v10.9 software from Schrodinger Inc. All calculations utilized the M06-2X meta-GGA functional with the D3 empirical correction for London dispersion forces.<sup>21,22</sup> All atoms were described by the 6-311G\*\*++ Pople basis set,<sup>23</sup> augmented with polarization and diffuse functions.

All calculations included a continuum solvent treatment described by the Polarizable Continuum Model (CPCM).<sup>24</sup>

Unless otherwise noted, we used solvent parameters matching tetrahydrofuran (dielectric constant = 7.6, probe radius = 2.52).

Vibrational frequency calculations were performed to confirm that all geometries are true minima (no negative eigenmodes of the Hessian) and to compute thermochemical properties such as enthalpy ( $H$ ), entropy ( $S$ ), and free energies ( $G$ ) at 298.15 K. Because librational modes are hindered in solvent media, we corrected our free energies by reducing translational and rotational entropy modes by 50%.

## ASSOCIATED CONTENT

### \* Supporting Information

The Supporting Information is available free of charge at <https://pubs.acs.org/doi/10.1021/acs.jpclett.4c02484>.

Figure S1: DFT-predicted binding energies at 300 K in  $\text{THF}$  solvent with  $\text{Na}$  counterions; Table S1: For the  $\text{Na}^+$  counterion in  $\text{THF}$ –Binding energies of  $\text{CO}_2$  binding and respective charges on the P atom and  $\text{BH}_3^-$  moiety in both reactant and product complexes (P–B and P–C bond orders are also displayed); Figure

S2: Thermogravimetric analysis of  $\text{LiPh}_2\text{PBH}_3\text{-CO}_2$  adducts computationally predicted NMR shifts using GIAO of  $\text{X}[\text{PPh}_2\text{BH}_3]$  reactant and product complexes coordinate geometries of all DFT-computed geometries  
(PDF)

## AUTHOR INFORMATION

### Corresponding Authors

Aleksandrs Prokofjevs – *Department of Chemistry, North Carolina Agricultural and Technical State University, Greensboro, North Carolina 27411, United States;*  
Email: [aprokofjevs@ncat.edu](mailto:aprokofjevs@ncat.edu)

William A. Goddard III – *Materials and Process Simulation Center, California Institute of Technology, Pasadena, California 91125, United States;*  [orcid.org/0000-0003-0097-5716](https://orcid.org/0000-0003-0097-5716); Email: [wag@caltech.edu](mailto:wag@caltech.edu)

### Authors

Aarya D. Riasati – *Materials and Process Simulation Center, California Institute of Technology, Pasadena, California 91125, United States*

Charles B. Musgrave III – *Materials and Process Simulation Center, California Institute of Technology, Pasadena, California 91125, United States;*  [orcid.org/0000-0002-3432-0817](https://orcid.org/0000-0002-3432-0817)

Nathaniel Yeboah – *Department of Chemistry, North Carolina Agricultural and Technical State University, Greensboro, North Carolina 27411, United States;*  [orcid.org/0009-0005-5403-9482](https://orcid.org/0009-0005-5403-9482)

Complete contact information is available at:

<https://pubs.acs.org/10.1021/acs.jpcllett.4c02484>

### Notes

The authors declare no competing financial interest.

## ACKNOWLEDGMENTS

We thank DOE BES for funding (SC 0022230).

## REFERENCES

- (1) Wuebbles, D. J.; Jain, A. K. Concerns About Climate Change and the Role of Fossil Fuel Use. *Fuel Process. Technol.* 2001, **71** (1-3), 99–119.
- (2) Boden, T. A.; Marland, G.; Andres, R. J. Global, Regional, and National Fossil-Fuel  $\text{CO}_2$  Emissions. *Carbon Dioxide Inf. Anal. Cent. Oak Ridge Natl. Lab. USA Oak Ridge TN Dep. Energy*, 2009. Accessed: April 23, 2024.
- (3) Hack, J.; Maeda, N.; Meier, D. M. Review on  $\text{CO}_2$  Capture Using Amine-Functionalized Materials. *ACS. Omega* 2022, **7** (44), 39520–39530.
- (4) Diemert, K.; Hahn, T.; Kuchen, W. Zur Kenntnis Des Natriumdiphenylphosphinoformiats  $\text{Ph}_2\text{PCOONa}$ . *Phosphorus, Sulfur Silicon Relat. Elem.* 1991, **60** (3-4), 287–294.
- (5) Musgrave, C. B.; Prokofjevs, A.; Goddard, W. A. Phosphine Modulation for Enhanced  $\text{CO}_2$  Capture: Quantum Mechanics Predictions of New Materials. *J. Phys. Chem. Lett.* 2022, **13** (48), 11183–11190.
- (6) Buß, F.; Mehlmann, P.; Mück-Lichtenfeld, C.; Bergander, K.; Dielmann, F. Reversible Carbon Dioxide Binding by Simple Lewis Base Adducts with Electron-Rich Phosphines. *J. Am. Chem. Soc.* 2016, **138** (6), 1840–1843.
- (7) Xu, Y. F.; Duchesne, P. N.; Wang, L.; et al. High-Performance Light-Driven Heterogeneous  $\text{CO}_2$  Catalysis with Near-Unity Selectivity on Metal Phosphides. *Nat. Commun.* 2020, **11**, 5149.
- (8) Welch, G. C.; San Juan, R. R.; Masuda, J. D.; Stephan, D. W. Reversible, Metal-Free Hydrogen Activation. *Science* 2006, **314**, 1124–1126.
- (9) Harhausen, M.; Fröhlich, R.; Kehr, G.; Erker, G. Reactions of Modified Intermolecular Frustrated P/B Lewis Pairs with Dihydrogen, Ethene, and Carbon Dioxide. *Organometallics* 2012, **31** (7), 2801–2809.
- (10) Dornhaus, F.; Bolte, M.; Lerner, H.-W.; Wagner, M. Phosphanylborohydrides: First Assessment of the Relative Lewis Basicities of  $[\text{BH}_3\text{PPh}_2]^-$ ,  $\text{CH}_3\text{PPh}_2$ , and  $\text{HPPPh}_2$ . *Eur. J. Inorg. Chem.* 2006, **2006**, 1777–1785.
- (11) Lebel, H.; Morin, S.; Paquet, V. Alkylation of Phosphine Boranes by Phase-Transfer Catalysis. *Org. Lett.* 2003, **5** (13), 2347–2349.
- (12) Barozzino Consiglio, G.; Queval, P.; Harrison-Marchand, A.; Mordini, A.; Lohier, J.-F.; Delacroix, O.; Gaumont, A.-C.; Gérard, H.; Maddaluno, J.; Oulyadi, H.  $\text{Ph}_2\text{P}(\text{BH}_3)\text{Li}$ : From Ditopicity to Dual Reactivity. *J. Am. Chem. Soc.* 2011, **133** (16), 6472–6480.
- (13) Lebel, H.; Morin, S.; Paquet, V. Alkylation of Phosphine Boranes by Phase-Transfer Catalysis. *Org. Lett.* 2003, **5** (13), 2347–2349.
- (14) Valentín, M.; Montes, E.; Adam, W. Counterion Effects in the Nucleophilic Substitution Reaction of the Acetate Ion with Alkyl Bromides in the Synthesis of Esters. *J. Chem. Educ.* 2009, **86** (11), 1315.
- (15) Buß, F.; Röthel, M. B.; Werra, J. A.; Rotering, P.; Wilm, L. F.; Daniliuc, C. G.; Löwe, P.; Dielmann, F. Tris(tetramethylguanidinyl)phosphine: The Simplest Non-ionic Phosphorus Superbase and Strongly Donating Phosphine Ligand. *Chem. Eur. J.* 2022, **28**, No. e202104021.

(16) Buß, F.; Mehlmann, P.; Mück-Lichtenfeld, C.; Bergander, K.; Dielmann, F. Reversible Carbon Dioxide Binding by Simple Lewis Base Adducts with Electron-Rich Phosphines. *J. Am. Chem. Soc.* 2016, 138 (6), 1840–1843.

(17) Mehlmann, P.; Mück-Lichtenfeld, C.; Tan, T. T.; Dielmann, F. Tris (imidazolin-2-ylidenamino) phosphine: A Crystalline Phosphorus (III) Superbase That Splits Carbon Dioxide. *Chem. Eur. J.* 2017, 23 (25), 5929–5933.

(18) Diemert, K.; Hahn, T.; Kuchen, W.; Tommes, P. Darstellung und Reaktionen Einiger Lithiumphosphinoformate R<sub>2</sub>PCOOLi und RHPCOOLiAb Initio-Rechnungen im System H<sub>2</sub>PCOOH<sub>3</sub>/CO<sub>2</sub>. *Phosphorus, Sulfur Silicon Relat. Elem.* 1993, 83 (1–4), 65–76.

(19) Stankevič, M.; Pietrusiewicz, K. M. An Expedient Reduction of sec-Phosphine Oxides to sec-Phosphine-Boranes by BH<sub>3</sub>·SMe<sub>2</sub>. *Synlett* 2003, 2003 (7), 1012–1016.

(20) Jaska, C. A.; Lough, A. J.; Manners, I. Linear Hybrid Aminoborane/Phosphinoborane Chains: Synthesis, Proton-Hydride Interactions, and Thermolysis Behavior. *Inorg. Chem.* 2004, 43 (3), 1090–1099.

(21) Zhao, Y.; Truhlar, D. G. Density Functionals with Broad Applicability in Chemistry. *Acc. Chem. Res.* 2008, 41 (2), 157–167.

(22) Grimme, S.; Antony, J.; Ehrlich, S.; Krieg, H. A Consistent and Accurate Ab Initio Parametrization of Density Functional Dispersion Correction (DFT-D) for the 94 Elements H–Pu. *J. Chem. Phys.* 2010, 132 (15), 154104.

(23) Hehre, W. J.; Ditchfield, K.; Pople, J. A. Self-Consistent Molecular Orbital Methods. XII. Further Extensions of GaussianType Basis Sets for Use in Molecular Orbital Studies of Organic Molecules. *J. Chem. Phys.* 1972, 56 (5), 2257–2261.

(24) Takano, Y.; Houk, K. N. Benchmarking the Conductor-like Polarizable Continuum Model (CPCM) for Aqueous Solvation Free Energies of Neutral and Ionic Organic Molecules. *J. Chem. Theory Comput.* 2005, 1 (1), 70–77.